

Fabrication of a Multilayered Gradient Self-Crosslinking Chitosan Hydrogel by a Controlled Freeze-Melting-Neutralization Method

Yongxiang Xu, Jianmin Han, and Hong Lin*

Department of Dental Materials, Peking University School and Hospital of Stomatology, Beijing 100081, China;
National Engineering Laboratory for Digital and Material Technology of Stomatology, Beijing 100081, China

Chitosan (CS) physical hydrogels without external cross-linkers are attractive materials for biomedical applications owing to their biodegradability and biocompatibility. In the present study, multilayered self-crosslinking CS hydrogels with gradient structures were fabricated by a controlled freeze-melting-neutralization method. The microstructure and properties of hydrogels can be adjusted by changing the relationship between melting rate and neutralizing rate of frozen CS samples through not only the freezing temperature and concentration of the CS solution but also the concentration and temperature of the NaOH neutralization solution. Using bovine serum albumin as a model protein, *in vitro* drug release studies indicated that the release profile was influenced by the CS hydrogel microstructure. These results suggest that multilayered self-crosslinking CS hydrogels can be fabricated by a simple freeze-melting-neutralization method and can serve as effective scaffolds for tissue engineering.

Keywords: Chitosan, Physical Hydrogels, Multilayered Gradient Structure, Freeze-Melting-Neutralization Method.

1. INTRODUCTION

Hydrogels are cross-linked three-dimensional polymer networks that are useful as biomaterials owing to their high water content, which makes them compatible with most living tissues^{1–3} as tissue barriers^{4–6} and tissue engineering scaffolds.^{7–9} Tissue-like structure/properties are key features of gels in medical applications.¹⁰ For example, gradient hydrogels with special spatial configurations can be used to mimic the architecture of tissues such as skin and bone.¹¹ Hydrogels with excellent mechanical properties have been fabricated using sliding crosslinking agents and double network hydrogels.^{12,13} In addition, injectable and environmental stimulus-responsive hydrogels have been developed for controlled, localized drug delivery.¹⁴

The chitosan (CS) hydrogel is especially attractive for biomedical applications due to its biocompatibility, low toxicity, biodegradability, and sterility.^{15–17} CS is a linear, semi-crystalline, naturally occurring polysaccharide composed of randomly distributed β -(1-4)-linked D-glucosamine and N-Acetyl-D-glucosamine units. The primary aliphatic amines of CS can be protonated under

acidic conditions ($pK_a = 6.3$), which renders the molecule fully soluble.¹⁸

CS can be induced to form a hydrogel in aqueous solutions by increasing pH or extruding the solution into a nonsolvent without adding other polymers or complexing molecules.^{19–23} CS hydrogels are formed via crystallites, hydrogen bonds, and hydrophobic interactions using the freeze-gelation technique, in which a CS solution is introduced into a mold and subjected to controlled freezing.²⁴ The frozen CS is then placed in a gelation solution of ethanol and sodium hydroxide below the CS freezing temperature to induce gelation.^{19,20}

Multi-member hydrogels have been developed by exploiting the pH-dependent solubility of CS under mild conditions.²⁵ A mixture of CS and 1,2-propanediol was introduced into a mold and evaporated at 55 °C to form an alcohol gel that was submerged in an NaOH solution to neutralize the CS amino groups and extrude 1,2-propanediol. The disruption of gelation led to the formation of a multilayered hydrogel that could be used to encapsulate molecules for the co-delivery of multiple drugs, pulse-like delivery of a specific payload, or as chondrocytic cell bioreactors.²⁶ Other multilayered hydrogels

* Author to whom correspondence should be addressed.

have also been fabricated either by sequential gel formation around pre-formed inner parts or by periodic precipitation using single-opening and semi-permeable membrane cylindrical molds.^{27,28}

Designing and fabricating scaffolds that mimic the architecture of tissue are a major challenge in the field of regenerative medicine.²⁹ Most tissues, such as skin, bone, and tooth are multilayered gradient structures. For example, teeth comprise enamel, dentin, and cementum surrounding the dental pulp, with each layer exhibiting a different microstructure.³⁰

In the present study, we fabricated a multi-layered gradient CS hydrogel that mimics the gradient structure of tissues by the physical gelation of pure CS without toxic covalent linker molecules. The hydrogel was processed based on the pH-dependent solubility of CS. Importantly, freezing/melting was introduced during the neutralization-gelation process of CS solution to adjust the microstructures of the different layers. The influence of the formation conditions on the final hydrogel structure and properties and on the release of protein is further discussed.

2. MATERIALS AND METHODS

2.1. Materials

Chitosan (CS, 116 cp) with a deacetylation degree of 95% was purchased from Golden-Shell Pharmaceutical Co. Ltd. (Zhejiang, China). Acetic acid, sodium hydroxide (NaOH), Bromothymol Blue, and bovine serum albumin (BSA) were purchased from Sinopharm Chemical Reagent Beijing Co., Ltd. (Beijing, China). All other reagents and solvents were of analytical grade and used without further purification.

2.2. Preparation of the CS Physical Hydrogel

2.2.1. CS Purification

CS was dissolved at 0.05% (w/v) in a stoichiometrically equivalent amount of aqueous acetic acid. After complete dissolution, the mixture was sequentially filtered through membranes with pore sizes of 3, 0.8, and 0.45 μm (Millipore, Billerica, MA, USA). The filtrate was precipitated with dilute ammonia (up to pH = 9) and centrifuged, then repeatedly rinsed with distilled, de-ionized water and centrifuged until a neutral pH was achieved before dispersion in water and freeze drying.

2.2.2. CS Hydrogel Formation

CS was dispersed in de-ionized water at different concentrations (C_{CS}) and a stoichiometrically equivalent amount of acetic acid was added. After complete dissolution, the solution was left to stand overnight without stirring for degassing at 4 °C. The solution was injected into a cylindrical mold (φ 9.0 \times 9.0 mm) and frozen at different temperatures (T_{CS}) for 24 h. The frozen CS solution was immediately immersed in 4 ml NaOH solution at different concentrations (C_{NaOH}) and temperatures (T_{NaOH}),

then gently shaken for 2 h to fully regenerate the free amine form of polymer chains. The hydrogel was removed from the NaOH solution and washed with 20 ml of 1 \times phosphate-buffered saline (PBS; pH 7.4) until a neutral pH was achieved.

2.3. Gelation of the CS Hydrogel

To clearly observe the gelation process, Bromothymol Blue was added to the CS solution. After freezing, the CS solution with indicator was fully immersed in NaOH solution in a cuboid quartz cuvette at room temperature. Images were captured from the side of the cuvette.

2.4. Characterization of CS Hydrogel Structure

The hydrogel was cut in half laterally and longitudinally. Images were captured before and after lyophilization. The microstructure of the cut sample was further characterized by scanning electron microscopy (EVO 18; Zeiss, Wetzlar, Germany).

2.5. Physico-Mechanical Characterization of the CS Hydrogel

2.5.1. Water Content (W_w)

CS hydrogel weight (W_h) was measured using an electronic balance after rapidly drying the surface with a filter paper. The dry weight (W_d) of the hydrogel was measured after lyophilization. W_w was calculated with the following formula.

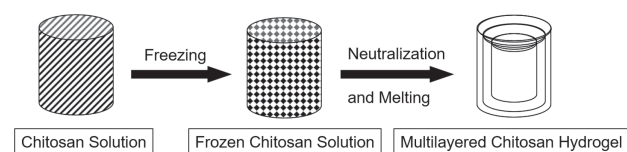
$$W_w = W_h - W_d$$

2.5.2. Mechanical Properties

Mechanical properties of CS hydrogels were determined by compression tests at a strain rate of 5 mm/min at room temperature using a universal material testing machine (model 5543A; Instron, Norwood, MA, USA).

2.5.3. Rheological Measurements

Rheological measurements were carried out at 37 °C with a rheometer (Physica MCR301; Anton Paar, Graz, Austria) operating with a plate–plate geometry (diameter: 25 mm). Rheological properties were investigated with dynamic mechanical experiments. Strain amplitude values were verified to ensure that all measurements were performed



Scheme 1. Schematic illustration of multilayered gradient CS hydrogel fabrication. The CS solution was first frozen, and then immersed in NaOH solution. Neutralization and melting of CS began at that time. The hydrogel was then removed from the NaOH solution and washed with PBS (pH = 7.4) until a neutral pH was achieved.

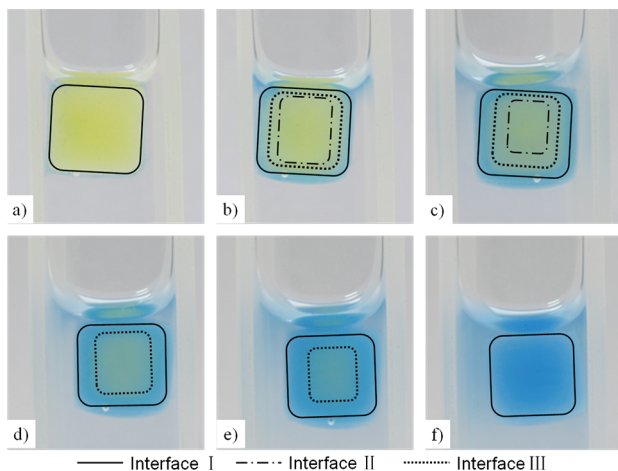


Fig. 1. Digital images of the gelation process of frozen CS solution at different time points ($C_{CS} = 20$ mg/ml, $T_{CS} = -20$ °C, $C_{NaOH} = 1.0$ M, and $T_{NaOH} = 23$ °C). Bromothymol Blue was added for visualization. According to the pH range, the blue color corresponded to hydrogel that was formed while the yellow color corresponded to ungelated parts. (1) Interface I: hydrogel-frozen CS solution boundary; (2) interface II: frozen-melted CS solution boundary; and (3) interface III: hydrogel-melted CS solution boundary.

within the linear viscoelastic range to obtain storage modulus (G') and a loss modulus (G'') independent of strain amplitude. Samples with a thickness of 1.5 mm were introduced between the plates.

2.6. Protein Release by the CS Hydrogel

The release of protein by the CS hydrogel was examined using BSA as a model molecule. BSA-loaded CS hydrogels were fabricated by freezing and neutralization using a cylindrical mold ($\varphi 9.0 \times 9.0$ mm). The release ratio of BSA in NaOH solution (R_0) and PBS solution (R_1) was recorded. Drug-loading efficiency (R_e) was calculated using the weight of BSA trapped by the hydrogel as a percentage of the total drug added, as follows.

$$R_e = (100 - R_0 - R_1)\%$$

The BSA-loaded CS hydrogel was immersed in 5 ml of $1 \times$ PBS (pH 7.4) at 37 °C with continuous shaking (60 rpm). At specific time intervals, a 1-ml aliquot of the medium was sampled and replaced with an equal volume of fresh PBS. BSA concentration was measured on a Microplate Reader (Model 680; Bio-Rad, Hercules, CA, USA) at 570 nm, and the cumulative amount of BSA released from the hydrogel was calculated from the standard curve of BSA. All experiments were repeated three times.

3. RESULTS AND DISCUSSION

3.1. Gelation of the CS Hydrogel

The formation of the multilayered gradient CS hydrogel is shown in Scheme 1.

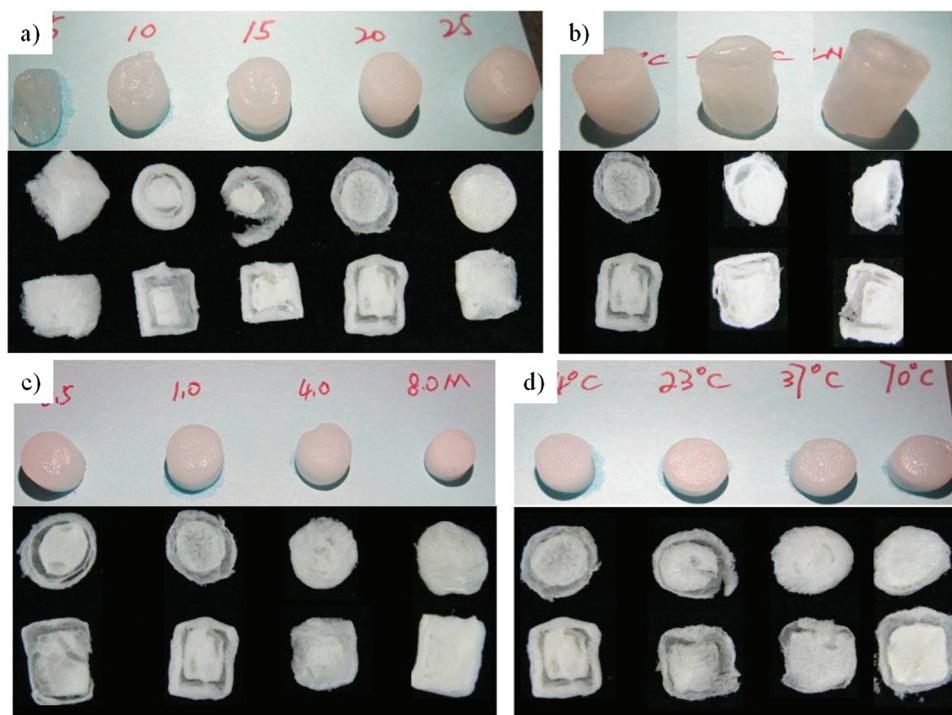


Fig. 2. Multi-layered hydrogel formation at $C_{CS} = 20$ mg/ml, $T_{CS} = -20$ °C, $C_{NaOH} = 1.0$ M, $T_{NaOH} = 4$ °C, excepting: (a) $C_{CS} = 5, 10, 15, 20,$ and 25 mg/ml; (b) $T_{CS} = -20$ °C, -80 °C, and -196 °C; (c) $C_{NaOH} = 0.5, 1.0, 4.0$ and 8.0 M; (d) $T_{NaOH} = 4, 23$ °C, 37 °C, and 70 °C. From top to bottom: hydrogels and lyophilized hydrogels cut in half (top and cross-sectional views).

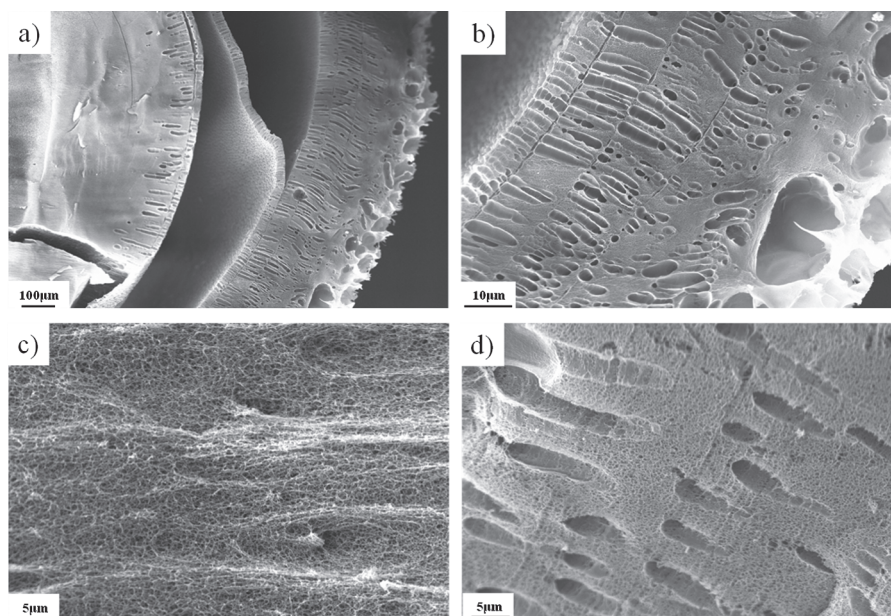


Fig. 3. Scanning electron micrographs of a CS hydrogel after lyophilization ($C_{CS} = 20$ mg/ml, $T_{CS} = -20$ °C, $C_{NaOH} = 1.0$ M, and $T_{NaOH} = 4$ °C). The hydrogel included three parts: the surface was composed of highly connected pores with diameters of 20–50 μm ; the middle had multiple layers consisting of nanofibers with radially oriented micro pores; and the core was a nanofiber structure.

The neutralization of CS NH_3^+ sites to NH_2 caused the loss of ionic repulsion between CS chains and induced crystallite formation, hydrogen bonding, and hydrophobic interactions. As a result, physical crosslinks were formed in the CS hydrogel.¹² Images of the gelation process are shown in Figure 1. After immersion in NaOH solution, neutralization and melting began synchronously at the surface of contact with the frozen CS solution. The contact area became a hydrogel layer (color change of the CS sample from yellow to blue in Fig. 1(a)) and served as interface I between the hydrogel and frozen CS solution. Almost simultaneously, interface II formed between the melting and frozen CS solutions and advanced to the inside of the sample (color change from dark yellow to light yellow in Fig. 1(b)).

Melting rate (R_m) and neutralization rate (R_n) of frozen CS solution were the two main factors affecting the structure of the CS hydrogel. The R_m is controlled by heat conduction and is mainly affected by T_{CS} and T_{NaOH} , while the R_n is related to OH^- concentration and diffusion and is influenced by C_{CS} and C_{NaOH} . As shown in Figure 1, R_m was higher than R_n under these conditions ($C_{CS} = 20$ mg/ml, $T_{CS} = -20$ °C, $C_{NaOH} = 1.0$ M, and $T_{NaOH} = 23$ °C). Consequently, interface I disappeared and interface III simultaneously appeared between the hydrogel and CS solution (Figs. 1(b) and (c)). The frozen CS solution eventually melted completely and interface II disappeared (Fig. 1(d)). Interface III formed gradually as OH^- diffused continuously into the CS solution (Fig. 1(e)), until all of the CS solution had gelled and the color turned from yellow to blue (Fig. 1(f)).

3.2. Multi-Layered Structures of CS Hydrogel

Bulk hydrogels were formed by simply freezing a CS solution in a suitable vessel and subsequently neutralizing the frozen samples. The multilayered architecture of CS hydrogels formed under different conditions before and after lyophilization at -20 °C is shown in Figure 2. Since the hydrogel will collapse when water is extracted by freeze-drying, the inter-layer space was larger in the dry than in the wet state. Some layers were destroyed during the cutting process. The hydrogels had an open pore microstructure with a high degree of interconnectivity after lyophilization.

Hydrogel volume increased slightly with increasing C_{CS} . No multilayered structure was observed at low C_{CS} (5 mg/ml) and no distinct layer was formed at high C_{CS} (25 mg/ml). Hydrogel volume increased with decreasing T_{CS} . Increasing C_{NaOH} favored a decrease in volume, with the multilayered structure eventually disappearing at



Fig. 4. Digital photographs of CS hydrogels with different shapes.

high concentrations ($C_{\text{NaOH}} = 8.0 \text{ M}$) due to high physical cross-linking density.

CS hydrogel structure was affected by both the freezing and gelling processes. Pore size and orientation can be controlled by the geometry of thermal gradients during freezing.²⁸ We therefore investigated the effects of R_m and R_n on the gelling process under different conditions (C_{CS} , T_{CS} , C_{NaOH} , and T_{NaOH}).

The surface hydrogel was composed of highly connected pores with diameters of 20–50 μm (Fig. 3). At surface of the frozen CS solution, R_m was slightly higher than R_n . However, the solubility of CS was prevented by the closing of the inner frozen CS prior to gelling. As a result, a structure was formed that was similar to the CS hydrogel formed from CS solution.²¹ The thickness of the outer layer increased with increasing T_{CS} and T_{NaOH} and

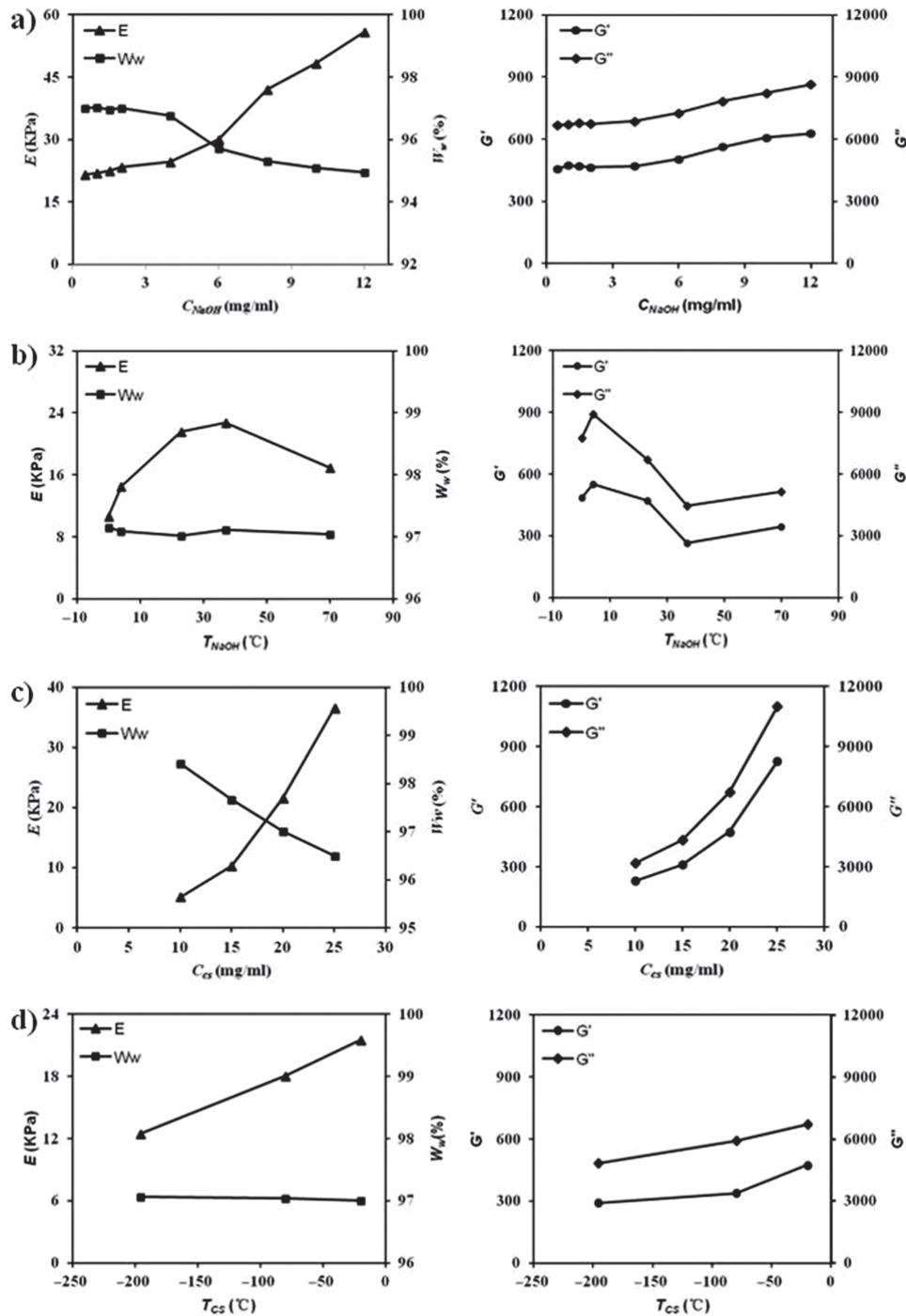


Fig. 5. Effect of fabrication conditions on W_w , E , G' , and G'' of CS hydrogels. (a) $C_{\text{CS}} = 10, 15, 20,$ and 25 mg/ml ; (b) $T_{\text{CS}} = -196^\circ\text{C}, -80^\circ\text{C},$ and -20°C ; (c) $C_{\text{NaOH}} = 10, 15, 20,$ and 25 mg/ml ; (d) $T_{\text{NaOH}} = 4^\circ\text{C}, 23^\circ\text{C}, 37^\circ\text{C},$ and 70°C .

decreasing of C_{NaOH} . The rough surface of the hydrogel favored cell adhesion and proliferation.

The middle part of the hydrogel consisting of multiple layers was composed of nanofibers with radially oriented micropores (Fig. 3(b)). Melting and neutralization of frozen CS were nearly synchronous in this part ($R_m = R_n$) and the hydrogel almost maintained the structure of frozen CS solution. These micropores were derived from ice crystals formed during the freezing process. The multilayered architecture arose from stress at the interface of the hydrogel and frozen solution.

A nanofiber structure without large pores was observed in the core hydrogel. It was formed from the CS solution after the frozen solution had melted under the limits of the outer layer hydrogel and no large pores were observed, since all the ice had melted before gelling occurred (Fig. 3(c)). Furthermore, the lower concentration of OH^- in the core hydrogel as compared to the surface resulted in a different structure between the two parts, although both were gelled from the CS solution.

Using specific templates, multilayered gradient CS hydrogels with different shapes were fabricated to mimic human tissues, such as disks and teeth (Fig. 4). Just as shown in Figure 3, the outer layer hydrogel could be used to mimic the enamel of tooth and the inner layer with oriented pores could be used to mimic the dentin of tooth.

Top: disks of different sizes; bottom: teeth.

3.3. Effect of Preparation Conditions on CS Hydrogel Properties

The physico-mechanical properties of CS scaffolds depend on their microstructure. The CS hydrogel was characterized in terms of W_w , compressive modulus (E), G' , and G'' .

W_w is an important parameter that represents the efficiency of oxygen and nutrient transfer within a scaffold.²⁹ As shown in Figure 5, the water content was >95% for all samples and decreased with increasing C_{CS} and C_{NaOH} . W_w was mostly unaffected by temperature (T_{CS} and T_{NaOH}). Furthermore, the hydrogels exhibit macropores, so they had significant water loss in the thawing process and under compression.

To investigate whether CS hydrogels can sustain mechanical loading, E was measured under different conditions. E increased markedly with increasing C_{CS} and C_{NaOH} , reaching a maximum value at $T_{\text{NaOH}} = 37^\circ\text{C}$. The hydrogels—which showed predominantly gel-like behavior—were also subjected to dynamic rheology measurements. Both G' and G'' increased with increasing C_{CS} and C_{NaOH} . Changes in mechanical properties (E , G' , and G'') were attributed to the solid content and crosslink density of the hydrogels. That is, the higher C_{NaOH} resulted from greater shrinkage and higher crosslink density, which enhanced the mechanical properties of the hydrogel.

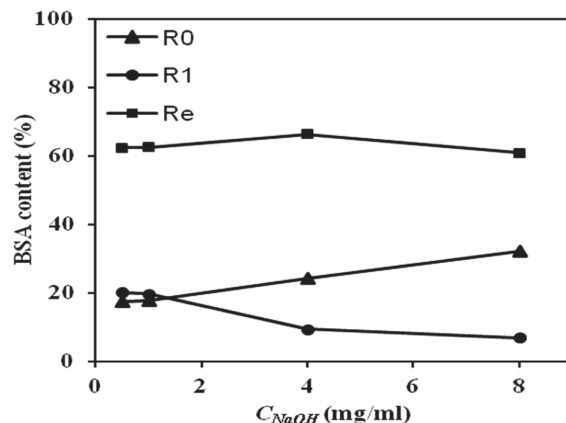


Fig. 6. BSA release in NaOH solution (R_0) and PBS solution (R_1) and payload BSA in CS hydrogels (R_e).

3.4. Release of BSA from CS Hydrogels

BSA was used as a model protein in this study to study the drug release of CS hydrogel via a physical entrapment method. A burst release of up to 40% of total BSA occurred during the gelling process; the amount of drug released into NaOH solution was $R_0 = 17.5\%–32.2\%$ and increased with increasing C_{NaOH} (Fig. 6) due to the acceleration of BSA diffusion and extrusion following the collapse of the hydrogel. BSA was released thereafter ($R_1 = 6.8\%–20.1\%$) in PBS solution and release rates decreased with increasing C_{NaOH} (Fig. 6).

The release rate of BSA primarily depended on hydrogel microstructure and the hydrodynamic kinetics of BSA. The hydrodynamic diameter of BSA is 7.2 nm, which is much less than the predicted mesh size of the CS hydrogel; as such, BSA molecules presumably diffused freely within the network. As shown in Figure 7, the higher crosslinking density at higher C_{NaOH} reduced the diffusion rate of BSA;

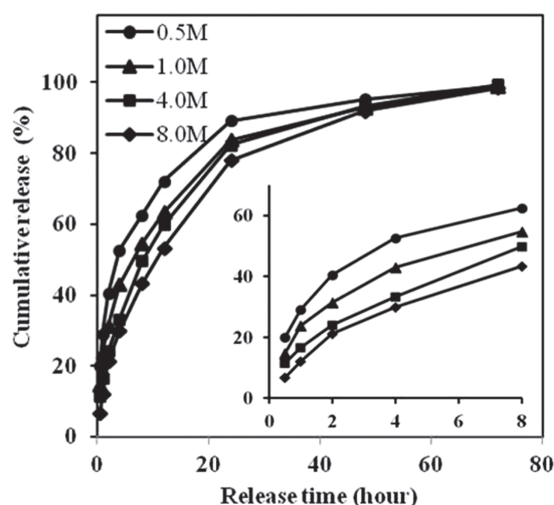


Fig. 7. Release profile of BSA from various CS hydrogels ($C_{\text{CS}} = 20\text{ mg/ml}$, $T_{\text{CS}} = -20^\circ\text{C}$, $T_{\text{NaOH}} = 4^\circ\text{C}$, $C_{\text{NaOH}} = 0.5, 1.0, 4.0, \text{ and } 8.0\text{ M}$) in $1 \times \text{PBS}$ (pH 7.4) at 37°C over 72 h.

this could also explain the release profile of payload BSA in the subsequent release (in PBS at 37 °C). Nearly all payload BSA was released after 72 h.

4. CONCLUSIONS

A multilayered self-crosslinking gradient CS hydrogel with different structures and properties was prepared via a controlled freeze-melting-neutralization method at different conditions (T_{CS} , T_{NaOH} , C_{CS} , and C_{NaOH}). The CS hydrogel had a multilayered structure composed of nanofibers with interconnected pores, and showed good mechanical properties and controlled BSA release. These results highlight the potential of multilayered self-crosslinking CS hydrogels as a scaffold for tissue engineering.

Acknowledgments: The work was supported by the National Natural Science Foundation of China (grant no. 81200814) and the National Key Technology R&D Program of China (grant no. 2012BAI22B03).

References and Notes

1. F. Croisier and C. Jerome, Chitosan-based biomaterials for tissue engineering. *Eur. Polym. J.* 49, 780 (2013).
2. O. Wichterle and D. Lim, Hydrophilic gels for biological use. *Nature* 185, 117 (1960).
3. J. Venkatesan, R. Jayakumar, S. Anil, E. P. Chalisserry, R. Pallela, and S. K. Kim, Development of alginate-chitosan-collagen based hydrogels for tissue engineering. *J. Biomater. Tissue Eng.* 5, 458 (2015).
4. Y. An and J. A. H. Hubbell, Intraarterial protein delivery via intimately-adherent bilayer hydrogels. *J. Control. Release* 64, 205 (2000).
5. J. A. Hubbell, Hydrogel systems for barriers and local drug delivery in the control of wound healing. *J. Control. Release* 39, 305 (1996).
6. E. A. Aksoy, U. A. Sezer, F. Kara, and N. Hasirci, Heparin/chitosan/alginate complex scaffolds as wound dressings: Characterization and antibacterial study against staphylococcus epidermidis. *J. Biomater. Tissue Eng.* 5, 104 (2015).
7. H. Dai, X. Li, Y. Long, J. Wu, S. Liang, X. Zhang, N. Zhao, and J. Xu, Multi-membrane hydrogel fabricated by facile dynamic self-assembly. *Soft Matter* 5, 1987 (2009).
8. S. L. Levengood and M. Zhang, Chitosan-based scaffolds for bone tissue engineering. *J. Mater. Chem. B Mater. Biol. Med.* 2, 3161 (2014).
9. P. Ma, Y. Fan, W. Wang, Z. Wu, B. Zhang, Q. Li, G. Qiu, and X. Weng, Characterization of thermosensitive and biocompatible property of chitosan/glycerophosphate hydrogel. *J. Biomater. Tissue Eng.* 5, 329 (2015).
10. B. V. Slaughter, S. S. Khurshid, O. Z. Fisher, A. Khademhosseini, and N. A. Peppas, Hydrogels in regenerative medicine. *Adv. Mater.* 21, 3307 (2009).
11. S. Sant, M. J. Hancock, J. P. Donnelly, D. Iyer, and A. Khademhosseini, Biomimetic gradient hydrogels for tissue engineering. *Can. J. Chem. Eng.* 88, 899 (2010).
12. J. P. Gong, Y. Katsuyama, T. Kurokawa, and Y. Osada, Double-network hydrogels with extremely high mechanical strength. *Adv. Mater.* 15, 1155 (2003).
13. Y. Okumura and K. Ito, The polyrotaxane gel: A topological gel by figure-of-eight cross-links. *Adv. Mater.* 13, 485 (2001).
14. Y. Qiu and K. Park, Environment-sensitive hydrogels for drug delivery. *Adv. Drug. Deliv. Rev.* 53, 321 (2001).
15. N. Bhattarai, J. Gunn, and M. Q. Zhang, Chitosan-based hydrogels for controlled, localized drug delivery. *Adv. Drug. Deliver. Rev.* 62, 83 (2010).
16. A. Domard, A perspective on 30 years research on chitin and chitosan. *Carbohydr. Polym.* 84, 696 (2011).
17. A. K. A. Silva, M. Juenet, A. Meddahi-Pelle, and D. Letourneur, Polysaccharide-based strategies for heart tissue engineering. *Carbohydr. Polym.* 116, 267 (2015).
18. G. Berth, H. Dautzenberg, and M. G. Peter, Physico-chemical characterization of chitosans varying in degree of acetylation. *Carbohydr. Polym.* 36, 205 (1998).
19. M. H. Ho, P. Y. Kuo, H. J. Hsieh, T. Y. Hsien, L. T. Hou, J. Y. Lai, and D. M. Wang, Preparation of porous scaffolds by using freeze-extraction and freeze-gelation methods. *Biomaterials* 25, 129 (2004).
20. C. Y. Hsieh, S. P. Tsai, M. H. Ho, D. M. Wang, C. E. Liu, C. H. Hsieh, H. C. Tseng, and H. J. Hsieh, Analysis of freeze-gelation and cross-linking processes for preparing porous chitosan scaffolds. *Carbohydr. Polym.* 67, 124 (2007).
21. K. Y. Lee and D. J. Mooney, Hydrogels for tissue engineering. *Chem. Rev.* 101, 1869 (2001).
22. A. Montebault, C. Viton, and A. Domard, Rheometric study of the gelation of chitosan in aqueous solution without cross-linking agent. *Biomacromolecules* 6, 653 (2005).
23. J. K. F. Suh and H. W. Matthew, Application of chitosan-based polysaccharide biomaterials in cartilage tissue engineering: A review. *Biomaterials* 21, 2589 (2000).
24. M. Dash, F. Chiellini, R. M. Ottenbrite, and E. Chiellini, Chitosan—A versatile semi-synthetic polymer in biomedical applications. *Progress in Polymer Science* 36, 981 (2011).
25. S. Ladet, L. David, and A. Domard, *Nature* 452, 76 (2008).
26. S. G. Ladet, K. Tahiri, A. S. Montebault, A. J. Domard, and M. T. Corvol, Multi-membrane hydrogels. *Biomaterials* 32, 5354 (2011).
27. A. Dhanasingh and J. Groll, Polysaccharide based covalently linked multi-membrane hydrogels. *Soft Matter* 8, 1643 (2012).
28. J. Nie, W. Lu, J. Ma, L. Yang, Z. Wang, A. Qin, and Q. Hu, Orientation in multi-layer chitosan hydrogel: Morphology, mechanism, and design principle. *Sci. Rep.* 5, 7635 (2015).
29. R. Langer and J. Vacanti, Tissue engineering: The design and fabrication of living replacement devices for surgical reconstruction and transplantation. *Science* 260, 920 (1993).
30. C. S. Young, S. Terada, J. P. Vacanti, M. Honda, J. D. Bartlett, and P. C. Yelick, Tissue engineering of complex tooth structures on biodegradable polymer scaffolds. *J. Dent. Res.* 81, 695 (2002).

Received: 2 December 2015. Accepted: 14 December 2015.